# NUMERICAL STUDY OF COMBINED CONVECTION HEAT TRANSFER FOR THERMALLY DEVELOPING UPWARD FLOW IN A VERTICAL CYLINDER

by

***Hussein A. MOHAMMED and Yasin K. SALMAN***

Original scientific paper
UDC: 532.517.2:519.876.5
BIBLID: 0354-9836, *12* (2008), 2, 89-102
DOI: 10.2298/TSCI0802089M

*The problem of the laminar upward mixed convection heat transfer for thermally developing air flow in the entrance region of a vertical circular cylinder under buoyancy effect and wall heat flux boundary condition has been numerically investigated. An implicit finite difference method and the Gauss elimination technique have been used to solve the governing partial differential equations of motion (Navier Stocks equations) for two-dimensional model. This investigation covers Reynolds number range from 400 to 1600, heat flux is varied from 70 W/m$^2$ to 400 W/m$^2$.*
*The results present the dimensionless temperature profile, dimensionless velocity profile, dimensionless surface temperature along the cylinder, and the local Nusselt number variation with the dimensionless axial distance $Z^+$. The dimensionless velocity and temperature profile results have revealed that the secondary flow created by natural convection have a significant effect on the heat transfer process. The results have also shown an increase in the Nusselt number values as the heat flux increases. The results have been compared with the available experimental study and with the available analytical solution for pure forced convection in terms of the local Nusselt number. The comparison has shown satisfactory agreement.*

Key words: *numerical combined convection, thermally developing flow, finite difference, vertical cylinder*

## Introduction

Combined forced and free convection in the entrance region of tubes occurs in many engineering installations such as heat exchangers, nuclear reactors, and solar collectors, *etc*. [1]. The internal heat transfer characteristics in mixed convection not only depend on whether the flow is hydrodynamically or thermally developing, laminar or turbulent, and on duct geometry, but also on whether the fluid is cooled or heated and on duct orientation (horizontal, inclined, and vertical upward or downward flow). In upward flow the natural and forced convection currents act in the same direction, the fluid will be accelerated in the region close to the tube wall due to mass continuity [2]. The full understanding of the prevailing velocity and temperature fields, as well as heat transfer coefficient, are necessary for the proper design and to estimate the magnitude of the thermal shock that some engineering systems wall will suffer from [3].

Confined mixed convection in ducts of different geometries has been studied extensively both experimentally and numerically. Early studies [4-8] for laminar mixed convection in circular ducts established the main differences between such flow fields and the corresponding

ones for forced convection in [4, 5]. Kemeny and Somers [6] studied experimentally the effect of properties variation on fully developed flow heat transfer and pressure drop in circular vertical tubes for water and oil as working fluids. Marner and McMillan [7] studied theoretically fully developed air flow in a vertical tube subjected to a sudden change in wall temperature (a step function). Zeldin and Schmidt [8] carried out experiments to determine the influence of gravity on the hydrodynamics and thermal characteristics of forced laminar flow in a long tube maintained at uniform temperature. They have also numerically predicted the velocity profiles and the Nusselt number with Gr/Re = –30 and were compared with their counterparts for pure forced convection and for air with Re = 500. Jackson *et al*. [9] presented comprehensive reviews of experimental, analytical, and numerical studies for vertical tubes. The substantial change of the Nusselt number in both developing and fully developed regions has been studied in [10, 11]. Wang *et al*. [12] investigated by a numerical analysis the effects of both hydrodynamic and thermal characteristics for laminar convection flow at low Peclet number in the thermal entrance region of vertical pipes by using finite difference method. Joye and Jacobs [13] investigated experimentally the flow patterns generated by buoyancy effects for water turbulent flow mixed convection heat transfer in a steam jacketed in a vertical tube. They found that the back flow of hot, large-scale turbulent eddies existed in both the boundary layer and the bulk flow near the entrance (top) of the heated section of the tube. Nesreddine *et al*. [14-15] have investigated the variable-property effect in laminar aiding and opposing mixed convection of air in vertical tubes and the effects of axial diffusion on laminar heat transfer with low Peclet numbers in the entrance region of thin vertical tubes. Laplante and Bernier [16] presented a numerical study of the effects of wall conduction on laminar water flow mixed convection in vertical pipes at a uniform wall heat flux boundary condition. EzEddine *et al*. [17] presented a numerical study of the interaction between thermal radiation and laminar mixed convection for ascending flows of emitting and absorbing gases such as $H_2O$, $CO_2$, and $H_2O$-$CO_2$ mixtures in vertical tubes. Su and Chung [18] presented a numerical study on the linear stability of mixed convection flow in a vertical pipe with constant heat flux with particular emphasis on the instability mechanism and the Prandtl number effect using liquid mercury, water, and oil as working fluids. Nguyen *et al*. [19-20] studied numerically the simultaneously developing upward transient, laminar flow of air, by using a full 3-D-transient-model and Boussinesq's assumptions, inside a uniformly heated vertical tube that is submitted to a uniform but time-dependent heat flux at the tube wall. The flow reversal effect and its location along the tube and the flow stability have been investigated. The results have shown that the flow seems to remain stable and unique up to the level of $Gr = 5 \cdot 10^5$ and $10^6$.

In the present work, the dimensionless velocity profile, the thermal field, and the heat transfer coefficient for a thermally developing laminar mixed convection air flow under upward buoyancy effect with constant wall heat flux boundary condition inside a vertical circular cylinder has been numerically studied. The results have also been compared with the experimental work done by the same authors [21].

## Mathematical modeling

### *Governing equations*

The present work is concerned with the numerical simulation of two-dimensional model to describe the mixed convection heat transfer in a vertical circular cylinder, with the configuration shown in fig. 1. The governing equations of motion have been developed based on the following assumptions: the flow is assumed to be laminar and upward (assisting flow), steady

state flow, fully developed velocity profile at the entrance of the test section, axially symmetric, constant wall heat flux boundary condition, and $C_p$ and $k$ are constants except the density in the buoyancy term, neglecting the viscous dissipation. The following differential equations representing continuity, conservation of momentum (Navier Stocks equations in both axial and radial directions), and conservation of energy equation have been written as follows [8].

Continuity equation:

$$\frac{\partial u}{\partial x} \quad \frac{v}{r} \quad \frac{\partial v}{\partial r} \quad 0 \tag{1}$$

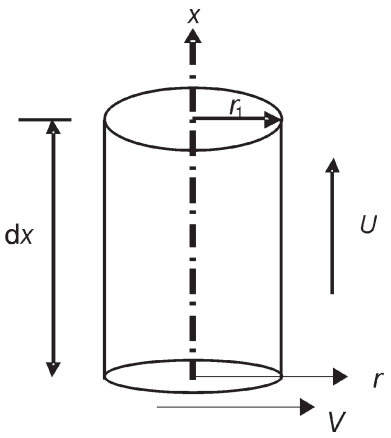


**Figure 1. Cylinder configuration**

Momentum equation in axial direction:

$$\rho \; v\frac{\partial u}{\partial r} \quad u\frac{\partial u}{\partial x} \qquad \frac{\partial p}{\partial x} \quad \rho g \quad \mu \; \frac{\partial^2 u}{\partial x^2} \quad \frac{1}{r}\frac{\partial u}{\partial r} \quad \frac{\partial^2 u}{\partial r^2} \quad 2 \; \frac{\partial u}{\partial x}\frac{\partial u}{\partial x} \quad \frac{\partial \mu}{\partial r} \; \frac{\partial v}{\partial x} \quad \frac{\partial u}{\partial r} \tag{2}$$

Momentum equation in radial direction:

$$\rho \; v\frac{\partial v}{\partial r} \quad u\frac{\partial v}{\partial x} \qquad \frac{\partial p}{\partial r} \quad \mu \; \frac{\partial^2 v}{\partial x^2} \quad \frac{1}{r}\frac{\partial v}{\partial r} \quad \frac{v}{r^2} \quad \frac{\partial^2 v}{\partial r^2} \quad 2 \; \frac{\partial \mu}{\partial r}\frac{\partial v}{\partial r} \quad \frac{\partial \mu}{\partial x} \; \frac{\partial v}{\partial x} \quad \frac{\partial u}{\partial r} \tag{3}$$

Energy equation:

$$v\frac{\partial t}{\partial r} \quad u\frac{\partial t}{\partial x} \quad \frac{k}{\rho c_p} \quad \frac{\partial^2 t}{\partial x^2} \quad \frac{1}{r}\frac{\partial t}{\partial r} \quad \frac{\partial^2 t}{\partial r^2} \tag{4}$$

The sign in the buoyancy term of eq. 2 (+) refers to upward flow and (–) for downward flow. In addition the integral continuity equation can be used in the following form:

$$\pi r_1^2 \rho_i u_m \quad \int_0^{r_i} 2\pi r \rho u \mathrm{d}r \tag{5}$$

The viscosity and density variation with temperature are taken to be:

$$\mu = \mu_i(C_1 + C_2 t - C_3 t^2) \tag{6}$$

and

$$\rho = \rho_i(C_4 - C_5 t + C_6 t^2) \tag{7}$$

where $C_1$, $C_2$, ……., $C_6$ are constant.

The boundary conditions, which have been used in the numerical solution, are:

– entry condition: $u = 2u_m[1 - (r/r_1)^2]$, $v = 0$, $p = p_i$, $t = t_i$
– cylinder axis: $v = 0$, $u/\ r = 0$, $t/\ r = 0$
– wall flow condition: $u = 0$, $v = 0$
– wall thermal condition: $q = k(\ t/\ r)r_1$ = constant heat flux.

By setting the following dimensionless parameters:

$$U \quad \frac{u}{u_{\mathrm{m}}},\ V \quad \frac{v}{u_{\mathrm{m}}},\quad R \quad \frac{r}{r_{\mathrm{i}}},\quad X \quad \frac{x}{r_{\mathrm{i}}},\quad p \quad \frac{p \quad p_{\mathrm{i}}}{\rho u_{\mathrm{m}}^2},\quad T \quad GC_5(t \quad t_{\mathrm{i}})$$

The physical properties viscosity and density variation, eq. (6) and (7), in dimensionless form become:

$$\mu = \mu_{\mathrm{i}}(Cc_1 + Cc_2 T - Cc_3 T^2) \tag{8}$$

$$\rho \quad \rho_{\mathrm{i}} \quad Cc_4 \frac{Cc_5}{G} T \quad \frac{Cc_6}{G} T^2 \tag{9}$$

where: $Cc_1 \quad C_1 \quad C_2 t_{\mathrm{i}} \quad C_3 t_{\mathrm{i}}^2,\ Cc_2 \quad (1/GC_5)(C_2 \quad 2C_3 t_{\mathrm{i}}),\ Cc_3 \quad C_3/G^2 C_5^2,$
$Cc_4 \quad (C_4 \quad C_5 t_{\mathrm{i}} \quad C_6 t_{\mathrm{i}}^2),\ Cc_5 \quad (2C_6 t_{\mathrm{i}}/C_5) - 1,\ Cc_6 = C_6/\mathrm{G}C_5^2$, and $G = r_{\mathrm{i}}^3 \mathrm{g}/\nu^2$.

By substituting the dimensionless parameters and eqs. (8) and (9), the eqs. (1)-(5) can be written in the following dimensionless form.

Continuity equation, eq. (1), becomes:

$$\frac{\partial U}{\partial X} \quad \frac{V}{R} \quad \frac{\partial V}{\partial R} \quad 0 \tag{10}$$

Momentum equation in axial direction, eq. (2), becomes:

$$V\frac{\partial U}{\partial R} \quad U\frac{\partial U}{\partial X} \quad \frac{\partial P}{\partial X} \quad \frac{1}{\mathrm{Re}^2}\frac{\rho}{\rho_{\mathrm{i}}}[GCc_4 \quad T(Cc_5 \quad Cc_6 T)]$$
$$\frac{1}{\mathrm{Re}} \quad Cc_1 \quad T(Cc_2 \quad Cc_3 T)\frac{\partial^2 U}{\partial X^2} \quad \frac{1}{R}\frac{\partial U}{\partial R} \quad \frac{\partial^2 U}{\partial R^2}$$
$$\frac{1}{\mathrm{Re}} \quad (Cc_2 \quad 2Cc_3 T)\,2\frac{\partial T}{\partial X}\frac{\partial U}{\partial X} \quad \frac{\partial T}{\partial R}\frac{\partial V}{\partial X} \quad \frac{\partial U}{\partial R} \tag{11}$$

Momentum equation in radial direction, eq. (3), becomes:

$$V\frac{\partial V}{\partial R} \quad U\frac{\partial V}{\partial X} \quad \frac{\partial P}{\partial R} \quad \frac{1}{\mathrm{Re}}[Cc_1 \quad T(Cc_2 \quad Cc_3 T)] \quad \frac{\partial^2 V}{\partial X^2} \quad \frac{1}{R}\frac{\partial V}{\partial R} \quad \frac{V}{R^2} \quad \frac{\partial^2 V}{\partial R^2}$$
$$+\frac{1}{\mathrm{Re}}[Cc_2 \quad 2Cc_3 T]\,2\frac{\partial T}{\partial R}\frac{\partial V}{\partial R} \quad \frac{\partial T}{\partial X}\frac{\partial V}{\partial X} \quad \frac{\partial U}{\partial R} \tag{12}$$

Energy equation, eq. (4), becomes:

$$V\frac{\partial T}{\partial R} \quad U\frac{\partial T}{\partial X} \quad \frac{1}{\mathrm{Re}\,\mathrm{Pr}} \quad \frac{\partial^2 T}{\partial X^2} \quad \frac{1}{R}\frac{\partial T}{\partial R} \quad \frac{\partial^2 T}{\partial R^2} \tag{13}$$

Integral continuity equation, eq. (5) becomes:

$$\frac{1}{2} \quad \int_0^1 UR \quad Cc_4 \quad \frac{Cc_5}{G} T \quad \frac{Cc_6}{G} T^2 \quad \mathrm{d}R \tag{14}$$

The boundary conditions in dimensionless form are:

– entry condition: $U = 2\,(1 - R^2)$, $V = 0$, $P = 0$, $T = 0$,
– cylinder axis: $V = 0$, $U/\ R = 0$, $T/\ R = 0$,
– wall flow condition: $U = 0$, $V = 0$, and
– wall thermal condition: $q = k\,(\partial T/\partial R)_{R\ 1}\,(v^2/r_1^4/C_5 g)$ = constant heat flux.

*Numerical solution*

In the thermal entrance length, the problem of air flow with constant physical properties except the density in buoyancy term is that the energy equation eq. (13) is coupled with the continuity and momentum eqs. (10)-(12). This enables the problem to be divided into two parts, the equation of energy can be solved to determine the temperature profile after which the continuity equation and momentum equation can be solved to determine the hydrodynamic characteristics of the entry length by using the temperature profile previously obtained from thermal calculations. In the following numerical approximation method, the energy equation will be solved by a direct implicit technique and the hydrodynamic part of the problem will be solved by means of extension to the linearized implicit finite difference technique. A rectangular grid was used with suffices "n", and "m" for the axial and radial directions, respectively. A uniform radial spacing has been used and the radial mesh points distributions along the cylinder were shown in fig. 2, but the marching procedure permitted a doubling of the axial step size at arbitrary location and any number of times. Basically, the unknown solution grid point is defined by suffices (n + 1, m) and the finite difference method is used to give sets of linear equations for the variable $U$, $V$, $P$, and $T$ at the unknown axial position "n + 1". Where the product of two unknowns occurs, linearity in the set of equations is achieved by putting one unknown at its value at the previous known step "n". The boundary conditions in finite difference form become:

– entry condition: $U_{1\,m} = 2[1 - (m - 1)^2/M^2]$, $V_{1\,m} = 0$, $P_{1\,m} = 0$, $T_{1\,m} = 0$,
– cylinder axis: $U_{n\,1} = U_{n\,2}$ , $V_{n\,1} = 0$ , $P_{n\,1} = P_{n\,2}$, $T_{n\,1} = T_{n\,2}$,
– wall flow condition: $U_{n\,M+1} = 0$, $V_{n\,M+1} = 0$, and
– wall thermal condition: $T_{n\,M+1} = T_{n\,M} + (qr_1^4 C_5 g/v^2 Mk)$.

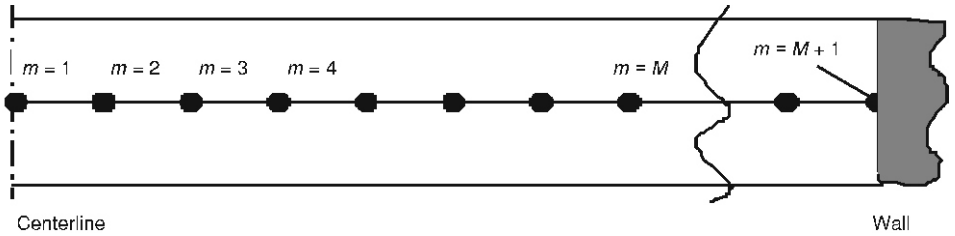


**Figure 2. Radial mesh points**

*Computational method and simulation program*

In the present numerical work a computational model has been developed to study the effect of various parameters such as the heat flux and the Reynolds number on the velocity and temperature profiles and on the heat transfer coefficient in a vertical circular cylinder. The computer program method to solve the above equation is as follows: energy equation, eq. (13), (for temperature) has been written for each radial position at first axial step. This gives a set of "M – 1" equations for the unknowns "T's" that were solved by Gauss elimination method.

Then, eq. (10)-(12) and with integral continuity equation, eq. (14), were similarly written and solved for the unknowns $U$, $V$, and $P$ and these gives "3M – 2" equations for $U$, $V$, and $P$ unknowns. The known values of $T$, $U$, $V$, and $P$ where then used as input data to solve the next axial step. The introduction of second derivative of velocity and temperature in the axial direction means that three axial positions were involved in the finite difference approximation, two positions (suffices "n – 1" and "n") were known and one (suffix "n + 1") was unknown. After solution of a given step, the old values at "n" and "n + 1" become the new values at "n – 1" and "n", respectively, and old "n – 1" data redundant. Knowing the temperature profiles from the numerical solution of energy, the mixing cup temperature and the local Nusselt number at any cross-section can be calculated. The mixing cup temperature at any cross-section is defined by:

$$t_{\mathrm{m}} \quad \frac{\int_0^{r_1} tur\,\mathrm{d}r}{\int_0^{r_1} ur\,\mathrm{d}r} \tag{15}$$

or, in dimensionless form:

$$T_{\mathrm{m}} \quad \frac{\int_0^1 TUR\,\mathrm{d}R}{\int_0^1 UR\,\mathrm{d}R} \tag{16}$$

The local Nusselt number at any cross-section is defined by:

$$\mathrm{Nu}_{\mathrm{x}} \quad \frac{qD}{k(t_{\mathrm{sx}} \quad t_{\mathrm{mx}})} \tag{17}$$

or, in dimensionless form:

$$\mathrm{Nu}_{\mathrm{x}} \quad \frac{\dfrac{\partial T}{\partial R}_{R\ 1}}{T_{\mathrm{sx}} \quad T_{\mathrm{mx}}} \tag{18}$$

where $T_{\mathrm{sx}}$ is the dimensionless local cylinder surface temperature and $T_{\mathrm{mx}}$ is the dimensionless local mixing cup temperature.

## Results and discussion

The numerical study has been mainly conducted to study combined convection heat transfer for upward air flow in a heated vertical cylinder. The dimensionless temperature profile evolution, dimensionless velocity profile evolution, variation of the surface temperature, and the axial local Nusselt number evolution along the cylinder have been investigated and presented in this section for different Reynolds numbers as well as different heat fluxes.

### *Dimensionless temperature profile*

The variation of temperature profiles along the vertical cylinder for selected runs are shown in figs. 3 and 4, which are represented for two Re numbers, Re = 400 and Re = 1600, with two different wall heat fluxes. The figures show a steep temperature gradient near the heated surface and the thickness of the thermal boundary layer gradually increases as the flow moves from cylinder inlet toward cylinder exit. It can be seen that there is relatively high temperature

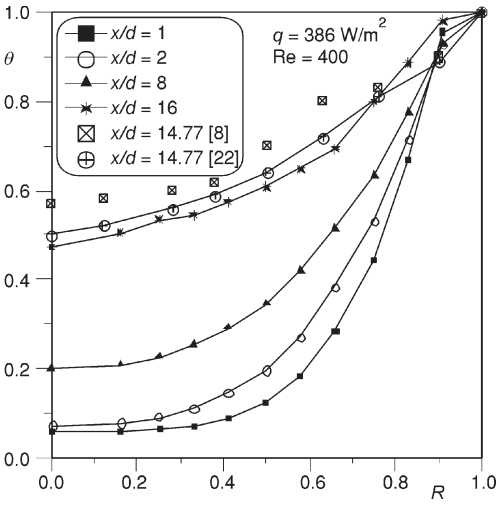


**Figure 3. Temperature profile development along the cylinder**

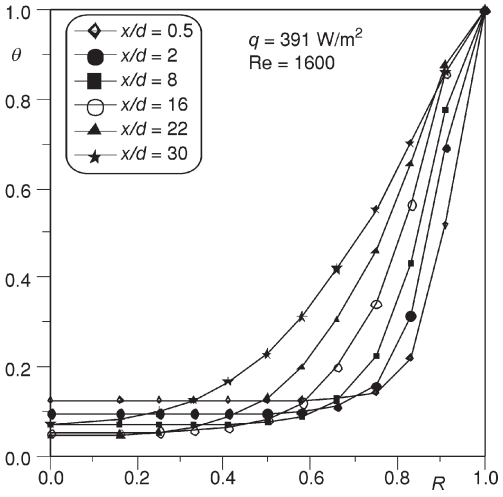


**Figure 4. Temperature profile development along the cylinder**

variation near the heated surface causes an appreciable density change, which creates a rapid growth of thermal boundary layer along cylinder length.

The temperature profiles along the cylinder axis, for Re = 1600 is shown in fig. 4. It was found from these figures that the thickness of the thermal boundary layer is lower than that obtained in fig. 3 as the forced convection is being the dominating factor on the heat transfer process.

### *Dimensionless velocity profile*

The dimensionless velocity profiles development along the cylinder axis, for Re = = 1600 and for different heat flux rates, are shown in figs. 5 and 6. For high Re number the profiles have revealed a small effect of buoyancy forces and show a similar to pure forced convection behavior. The maximum velocity occurs at dimensionless radial distance ($R$) equal to zero (cylinder centerline).

Figures 7 and 8 show the dimensionless axial velocity profiles development for Re = 400 and for various heat flux rates. The profiles at $x/d = 0$ are exactly similar to those for pure forced convection. However, in farther downstream, the centerline velocity decreases until it reaches a minimum value. The centerline velocity retreats gradually at $x/d = 30$ in fig. 8 but in fig. 7 the centerline velocity retreats gradually and starting earlier at $x/d = 20$. The maximum velocity does not occur at the cylinder centerline where as the maximum velocity moves tward the cylinder wall creates a concave down at the cylinder core. The central concavity of velocity profiles diminishes as $x/d$ increases but does not completely vanish. It can be seen that the profiles moves slightly toward the heated surface, and the maximum velocity for the last profiles at $x/d = 30$ occurs in fig. 8 at $R = = 0.58$ but it occurs at $R = 0.67$ in fig. 7.

It can be concluded from the results presented, that the distortion of velocity profiles increases as the heat flux increases due to free convection domination.The reason for these behaviors can be explained as follows: consider the air in the cross-section of the cylinder at some arbitrary location and let that $T_s > T_a$. The temperature of the air must increase in the radial direction; this leads to decrease the air density with $R$. Therefore, the effect of the gravitational body

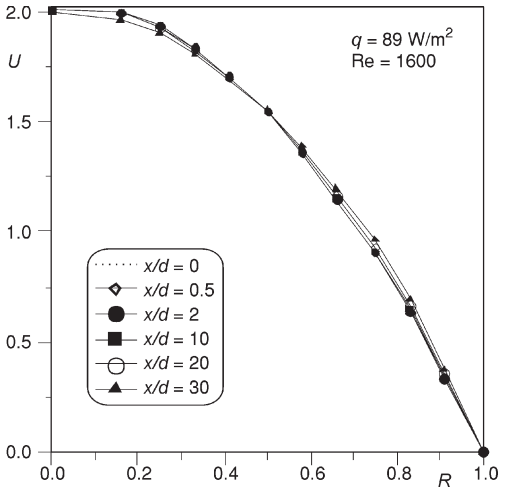


**Figure 5. Axial velocity profile development along the cylinder**

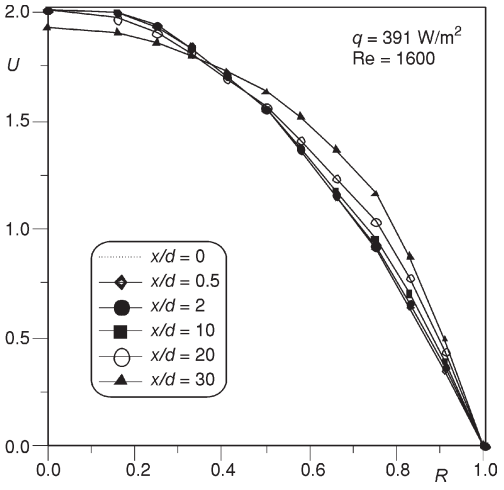


**Figure 6. Axial velocity profile development along the cylinder**

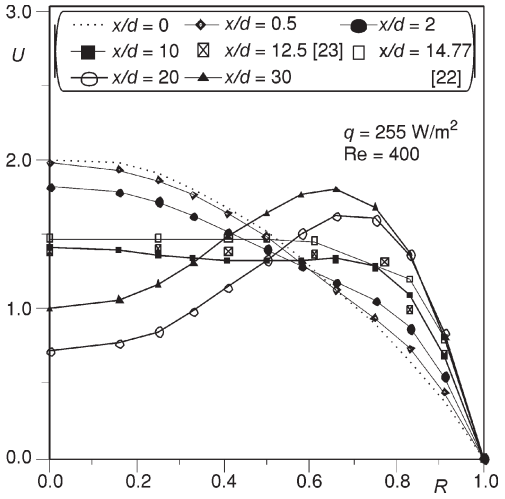


**Figure 7. Axial velocity profile development along the cylinder**

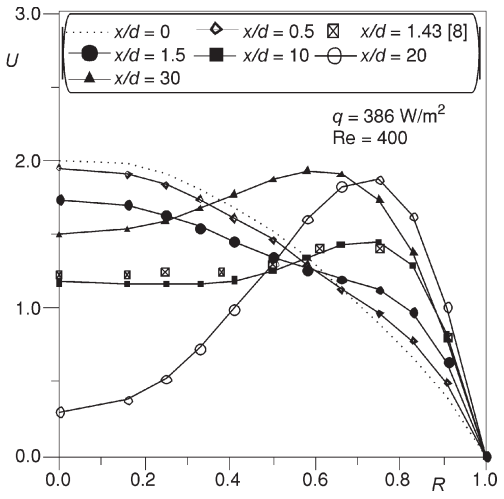


**Figure 8. Axial velocity profile development along the cylinder**

forces, which is proportional to the density, decreases in the radial direction. As a result, the air will tend to rise more rapidly near the walls and has a higher axial velocity and tends to slow up near the centerline and has axial velocity must be correspondingly lower. The air temperature approaches to $T_s$ as $x/d$ increases. Thus, the effect of the gravitational body forces cause significant changes in the velocity profiles as has been observed by Zeldin and Schmidt [8]. Figure 9 shows the axial velocity profiles, for Re = 200 and $q = 87$ W/m$^2$, the dimensionless velocity profiles development show a complete bias to the heated surface and the maximum velocity for the last profile at $x/d = 30$ occurs at $R = 0.59$. It is evident from this figure that the degree of central concavity decreases as Re number increases. The results have also revealed that the free convection has a tremendous effect of on the main forced convection.

A comparison, of the experimental results by Zeldin and Schmidt for laminar mixed convection for air in an isothermal vertical pipe [8]; and with the corresponding analytical results reported by Kakac [22] for isothermal flow, with the current corresponding numerical results shows good agreement for both velocity (figs. 7 and 8) and temperature (fig. 3) profiles except for the temperature profile near the heated region inlet ($x/d < 1$). However, as explained by Zeldin and Schmidt [8] the measured temperatures in that region were influenced by upstream conduction through the walls of the experimental setup.

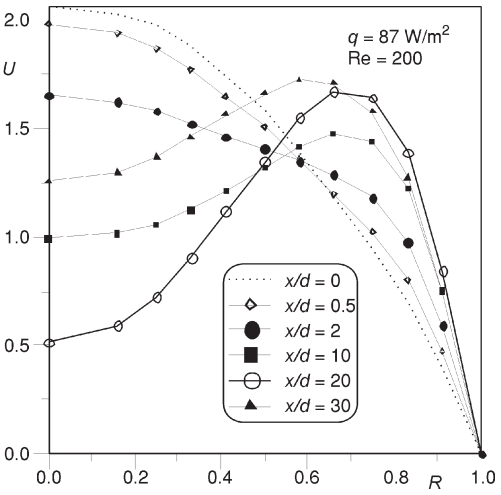


**Figure 9. Axial velocity profile development along the cylinder**

*Surface temperature*

The surface temperature distribution along a vertical cylinder is shown in figs. 10 and 11. The general shape is as follows: at the cylinder entrance the surface temperature gradually increases since the boundary layer thickness is zero after which it increases to reach maximum value at specific axial position due to the axial conduction, after that the surface temperature slightly decreases at cylinder exit due to the buoyancy effect. The surface temperature distribution along the cylinder, for different heat fluxes and for constant Reynolds numbers of 400 is shown in fig. 10. This figure reveals that the surface temperature increases with the increasing of the heat flux. This can be attributed to the developing of the thermal boundary layer faster due to buoyancy effect as the heat flux increases for the same Re number. A similar trends has been obtained for Re = 1600 (not shown). It has ben observed that the surface temperature values for high Re number are lower than for low Re number because of the forced convection domination on the heat transfer process.

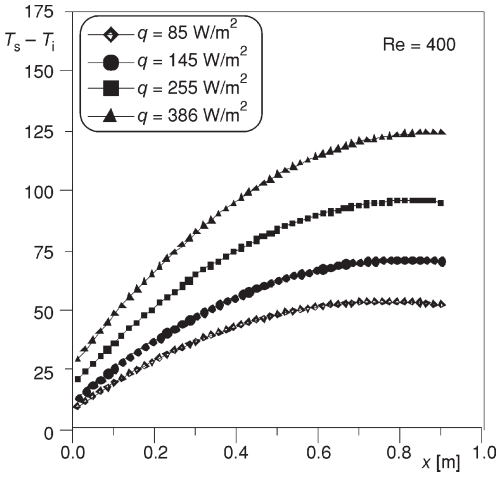


**Figure 10. Surface temperature variation along the cylinder**

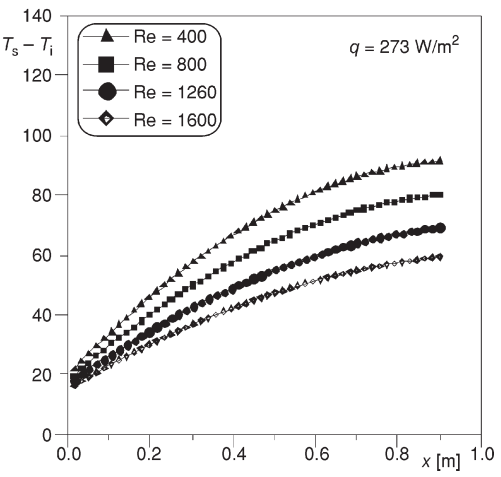


**Figure 11. Surface temperature variation along the cylinder**

Figure 11 shows the effect of Re number variation on the cylinder surface temperature for high heat flux 273 W/m$^2$. It is obvious that the increasing of Re number reduces the surface temperature, as the heat flux is kept constant. It is necessary to mention that as heat flux increases the surface temperature increases because of the free convection currents are becoming the dominating factors on the heat transfer process.

*Local Nusselt number ($Nu_x$)*

The axial evolution of the local Nusselt number ($Nu_x$) with the dimensionless axial distance ($Z^+$) for selected runs is shown in figs. (12)-(15). Figs. 12 and 13 show the effect of the heat flux variation on the $Nu_x$ distribution for Re = 400 and Re = 1600, respectively. It can be seen from these figures that the general variation of $Nu_x$ reveals that at the inlet of heated region are very high values because of the thickness of the thermal boundary layer is zero and it decreases continuously due to the thermal boundary layer develops and then near the exit of heated region the values increases due to the laminarization effect in the near wall region (buoyancy effect) and due to the upstream axial conduction in the solid walls.

It is clear that the $Nu_x$ value has the same shape for different heat fluxes at the cylinder entrance because the buoyancy effect is weak at that region, but beyond approximately at $Z^+ = 0.015$ the $Nu_x$ value increases as the heat flux increases. This is due to the increase in both the thermal boundary layer thickness and the surface to bulk air temperature difference which accompanies with an increase in the surface heat flux and that accelerate the development of the secondary flow in the cylinder downstream. While fig. 13 shows that there is no effect for increasing the heat flux on the $Nu_x$ values because of the forced convection domination on the heat transfer process (no secondary flow effect).

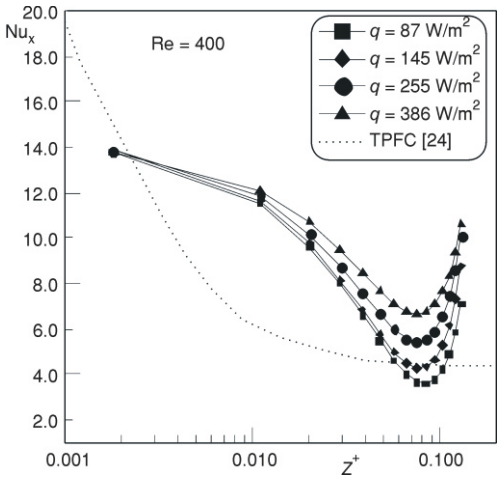


**Figure 12. Axial evolution of the local Nusselt number with the dimensionless axial distance**

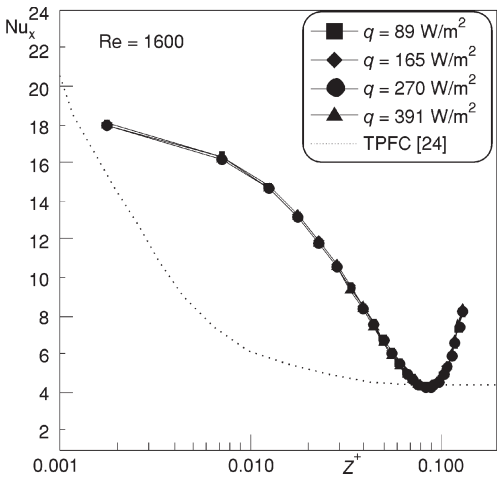


**Figure 13. Axial evolution of the local Nusselt number with the dimensionless axial distance**

Figures 14 and 15 show the effect of Re number variation on the $Nu_x$ for $q$ = 112 W/m$^2$ and $q$ = 273 W/m$^2$, respectively. These figures reveal that the effect of secondary flow is small at

the cylinder entrance (forced convection is dominant at this region) and the $Nu_x$ value increases in the cylinder downstream as Re number decreases because of the free convection is being dominant on the heat transfer process.

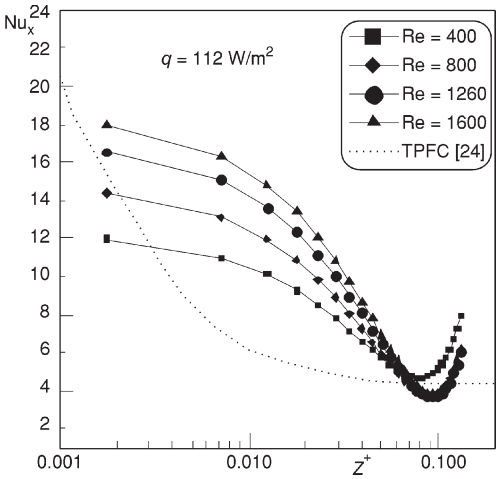


**Figure 14. Axial evolution of the local Nusselt number with the dimensionless axial distance**

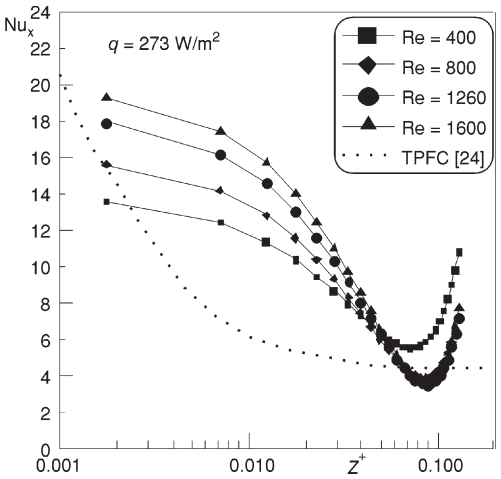


**Figure 15. Axial evolution of the local Nusselt number with the dimensionless axial distance**

The present numerical predictions of local Nusselt number have been compared with approximately corresponding sets of experiments done by the same authors [21], and with the corresponding analytical and numerical data available in the literature for the case of steady, laminar mixed convection upward flow of air in a uniformly heated vertical tube [20, 24] as shown in fig. 16. The figure reveals that the present numerical results follow the same trend as that reported in the literature in spit of there is a discrepancy about 15% between these studies which is accepted in heat transfer situations. This is may be attributed to some experimental uncertainties in the measurements of surface temperature and the accuracy of equipment used in the experimental work. Some of the assumptions used in the numerical method might be affected the results. The dotted curve in this figure represents theoretical pure forced convection curve (TPFC) based on constant property analysis of Shah and London [24]. As we can conclude that the mathematical model as well as the reliability of the chosen numerical method is appropriate for this case of study.

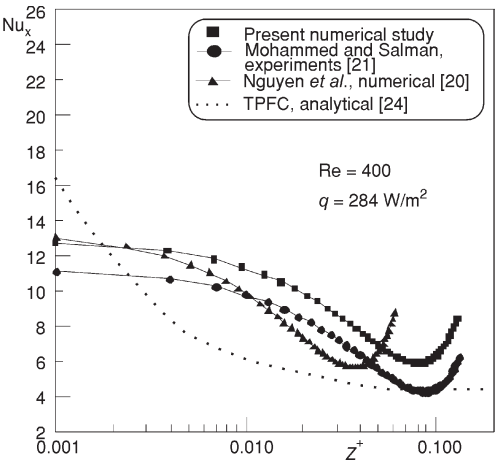


**Figure 16. Comparison of the axial local Nusselt number with the dimensionless axial distance with available literature**

## Conclusions

The following conclusions have been made from the present numerical investigation which shows a significant effect of combined free and forced convection on the temperature profile evolution, velocity profile evolution, the variation of the surface temperature, and axial evolution of the local Nusselt number along a heated vertical cylinder.

The temperature profile along the cylinder shows a steep profile near the heated surface.

For the same axial position and same Re number, the thermal boundary layer thickness increases as the heat flux increases because the effect of buoyancy force is accelerating the growth of the thermal boundary layer leading to heat transfer improvement.

For low Re number, the thermal boundary layer thickness is higher than that for high Re number, due to free convection domination on the heat transfer process.

Near the cylinder entrance the velocity profiles or different heat fluxes were found to be similar to those for pure forced convection behavior. But in the cylinder downstream the velocity profiles were distorted and a high degree of central concavity appeared by the action of buoyancy forces.

For high Re number, the velocity profiles does not change with the increasing of heat flux, from the pure forced convection trend and there is no effect of buoyancy forces. Nevertheless, for low Re number the velocity profile changes with increasing the heat flux.

The central concavity of velocity profiles diminishes as $x/d$ increases but does not completely vanish. The degree of central concavity decreases as Re number increases.

The variation of the surface temperature along the cylinder has the same trend and behavior as that obtained in the experimental work done by the same authors in their previous work [21].

At low Re number, the $Nu_x$ value increases with the increase of the heat flux in cylinder downstream due to increase of buoyancy effect. But at high Re number, there is no effect of increasing the heat flux on the $Nu_x$ values due to forced convection domination on the heat transfer process.

The $Nu_x$ value increases at cylinder downstream for low Re number due to the free convection domination on the heat transfer process.

The present computer model has been successfully validated by comparing the results as obtained for the development of the axial velocity component, and the development of the temperature profile as well as that of the axial local Nusselt number ($Nu_x$), to the corresponding experimental, analytical and numerical data available in the literature. The agreement between our results and others is reasonable. Therefore, we can conclude with confidence the appropriateness of the mathematical model as well as the reliability of the chosen numerical method.

## Nomenclature

$A_s$ – cylinder surface area, [$m^2$]
$C_1$, $C_4$ – constants, eqs. 6 and 7, [–]
$C_2$, $C_5$ – constants, eqs. 6 and 7, [$°C^{-1}$]
$C_3$, $C_6$ – constants, eqs. 6 and 7, [$°C^{-2}$]
$Cc_1$, $Cc_2$, $Cc_3$ – constants, eq. 8, [–]
$Cc_4$, $Cc_5$, $Cc_6$ – constants, eq. 9, [–]
$C_p$ – specific heat at constant pressure, [J $kg^{-1}°C^{-1}$]
$D$ – cylinder diameter, [m]
g – gravitational acceleration, [$ms^{-2}$]
Gr – Grashof number [$=g\beta D^3 (T_s - T_a)/\nu^2$ ), [–]
Gz – Graetz number (=RePr$D/L$), [–]
$h$ – heat transfer coefficient, [$Wm^{-2}°C^{-1}$]
$k$ – thermal conductivity, [$Wm^{-1}°C^{-1}$]
$L$ – cylinder length, [m]
$m$ – radial mesh point, [–]
$M$ – total radial mesh points, [–]
$n$ – axial mesh point, [–]

Nu – Nusselt number (= $hD/\kappa$), [–]
$P$ – dimensionless pressure at any cross-section (= $p - p_i/\rho u_m^2$), [–]
Pe – Peclet number (=RePr), [–]
Pr – Prandtl number (=$\mu C_p/k$), [–]
$q$ – heat flux, [$Wm^{-2}$]
$r$ – radial coordinate, [m]
$r_1$ – cylinder radius, [m]
$R$ – dimensionless radial coordinate, [–]
Re – Reynolds number (= $\rho vD/\mu$), [–]
$T$ – dimensionless temperature [= $GC_5(t - t_i)$], [–]
$T_A$, $T_B$ – constants, eq. (17), [–]
$T_i$ – inlet (ambient) temperature, [°C]
$T_s$ – surface temperature, [°C]
$t$ – air temperature at any point, [°C]
$t_m$ – mixing cup temperature over any cross--section, [°C]
$U$ – dimensionless axial velocity component (= $u/u_m$), [–]
$u$ – axial velocity component, [$ms^{-1}$]
$u_m$ – axial mean velocity, [$ms^{-1}$]
$V$ – dimensionless radial velocity component, (=$v/u_m$) [–]
$v$ – radial velocity component, [$ms^{-1}$]
$X$ – dimensionless axial coordinate (= $x/r_1$), [–]
$x$ – axial distance, [m]
$Z^+$ – dimensionless axial distance (= $x/D$RePr), [–]

*Greek letters*

$\beta$ – thermal expansion coefficient, [$K^{-1}$]
$\mu$ – dynamic viscosity, [$kgm^{-1}s^{-1}$]
$\nu$ – kinematic viscosity, [$m^2s^{-1}$]
$\rho$ – air density, [$kgm^{-3}$]
$\theta$ – dimensioless temperature [$(T - T_1)/(T_s - T_1)$], [–]

*Subscript*

a – air
i – inlet
s – surface
x – local

## References


[1] Bergles, A. E., Simonds, R. R., Combined Forced and Free Convection for Laminar Flow in a Horizontal Tube with Uniform Heat Flux, *Int. J. Heat and Mass Transfer, 14* (1971), 12, pp.1989-2000
[2] Aung, W., Mixed Convection in Internal Flow, in: Handbook of Single-Phase Convective Heat Transfer (Eds. S. Kakac, R. K. Shah, W. Aung), John Wiley and Sons, Inc., New York, USA, 1987, pp. 15.1-15.51
[3] Yousef, W. W., Tarasuk, J. D., Free Convection Effects on Laminar Forced Convective Heat Transfer in a Horizontal Isothermal Tube, *J. Heat Transfer, ASME Trans., 104* (1982), 2, pp. 145-152
[4] Hallman, T. M., Combined Forced and Free Laminar Heat Transfer in Vertical Tubes with Uniform Heat Generation, *J. Heat Transfer, ASME Trans., 78* (1956), 8, pp. 1831-1841
[5] Mori, Y., *et al*., Forced Convective Heat Transfer in Uniformly Heated Horizontal Tubes, *J. Heat and Mass Transfer, 9* (1966), 5, pp. 453- 463
[6] Kemeny, G. A., Somers, E. V., Combined Free and Forced Convective Flow in Vertical Circular Tubes – Experiments with Water and Oil, *ASME paper,* No. 61-WA-161 (1961), pp. 1-7
[7] Marner, W. J., McMillan, H. K., Combined Free and Forced Convection Laminar in a Vertical Tube with Constant Wall Temperature, *J. Heat Transfer, ASME Trans., 92* (1970), Ser. C(4), pp. 559-561
[8] Zeldin, B., Schmidt, F. W, Developing Flow with Combined Forced-Free Convection in an Isothermal Vertical Tube, *J. Heat Transfer, ASME Trans., 94* (1972), Ser. C(2), pp. 211-223
[9] Jackson, J. D., Cotton, M. A., Axcell, B. P., Studies of Mixed Convection in Vertical Tubes, *Int. J. Heat and Fluid Flow, 10* (1989), 1, pp. 2-15
[10] Barozzi, G. S., Zanchini, E., Mariotti, M., Experimental Investigation of Combined Forced and Free Convection in Horizontal and Inclined Tubes, *Meccanica, 20* (1985), 1, pp. 18-27
[11] Orfi, J., Galanis, N., Nguyen, C. T., Simultaneous Development of a Laminar Flow Inside an Inclined Tube with Mixed Convection (in French), *Revue Générale de Thermique, 36* (1997), 2, pp. 83-92
[12] Wang, M., Tsuji, T., Nagano, Y., Mixed Convection with Flow Reversed in the Thermal Entrance Region of Vertical Pipes, *J. Heat Transfer, ASME Trans., 37* (1994), 15, pp. 2305-2319
[13] Joye, D. D., Jacobs, S. W., Back Flow in the Inlet Region of Opposing Mixed Convection Heat Transfer in a Vertical Tube, *Proceedings*, 10th International Heat Transfer Conference, Brighten, UK, 1994, paper 12-NM-26, pp. 489-494
[14] Nesreddine, H., Galanis, N., Nguyen, C. T., Variable-Property Effects in Laminar Aiding and Opposing Mixed Convection of Air in Vertical Tubes, *Numer. Heat Transf., Part A, 31* (1997), 1, pp. 53-69

[15] Nesreddine, H., Galanis, N., Nguyen, C. T., Effects of Axial Diffusion on Laminar Heat Transfer with Low Peclet Numbers in the Entrance Region of Thin Vertical Tubes, *Numer. Heat Transf., Part A, 33* (1998), 5, pp. 247-266
[16] Laplante, G., Bernier, M. A., Opposing Mixed Convection in Vertical Pipes with Wall Heat Conduction, *Int. J. Heat and Mass Transfer, 40* (1997), 15, pp. 3527-3536
[17] EzEddine, S., Anouar, S., Mohamed Salah, S., Combined Gas Radiation and Laminar Mixed Convection in Vertical Circular Tubes, *Int. J. Heat and Fluid Flow, 24* (2003), 5, pp. 736-746
[18] Su, Y. C., Chung, J. N., Linear Stability Analysis of Mixed Convection Flow in a Vertical Pipe, *Journal of Fluid Mechanics, 422* (2004), 11, pp. 141-166
[19] Nguyen, C. T., *et al*., Transient Laminar Mixed Convection Flow in a Vertical Tube under High Grashof Number Condition, *J. Heat Transfer, ASME Trans., 21* (2004), 3, pp. 133-139
[20] Nguyen, C. T., *et al*., Numerical Investigation of Flow Reversal and Instability in Mixed Laminar Vertical Tube Flow, *Int. J. Thermal Sciences, 43* (2004), 3, pp. 797-808
[21] Mohammed, H. A; Salman, Y. K., Combined Natural and Forced Convection Heat Transfer for Assisting Thermally Developing Flow in a Uniformly Heated Vertical Circular Cylinder, *Int. J. Communications in Heat and Mass Transfer, 34* (2007), 4, pp. 474-491
[22] Voicu, I., *et al*., Mixed Convection in a Vertical Double Pipe Heat Exchanger, *Int. J. Thermal Sciences, 46* (2007), 6, pp. 540-550
[23] Kakac, S., Shah, R. K., Aung, W., Handbook of Single Phase Convective Heat Transfer, John Wiley and Sons Inc., New York, USA, 1987
[24] Shah, R. K., London, A. L., Laminar Flow Forced Convection in Ducts, Advances in Heat Transfer, Supplement 1, Academic Press, New York, USA, 1978

Authors' addresses:

*H. A. Mohammed*
University Tenaga Nasional, College of Engineering,
Mechanical Engineering Department
Km7, Jalan Kajang – Puchong,
43009 Kajang, Selangor, Malaysia

*Y. K. Salman*
Baghdad University, College of Engineering,
Nuclear Engineering Department
Baghdad, Al-Jaderyia, Iraq

Corresponding author H. A. Mohammed
E-mail: hussein@uniten.edu.my

Paper submitted: November 13, 2006
Paper revised: January 24, 2007
Paper accepted: September 27, 2007